A Comprehensive Mechanistic Picture of the Isomerizing Alkoxycarbonylation of Plant Oils

Philipp Roesle,[†] Lucia Caporaso,*[,‡] Manuel Schnitte,[†] Verena Goldbach,[†] Luigi Cavallo,[‡,§] and Stefan Mecking*[,†]

[†]Chair of Chemical Materials Science, Department of Chemistry, University of Konstanz, 78464 Konstanz, Germany

[‡]Department of Chemistry, University of Salerno, Via Giovanni Paolo II, 84084-Fisciano, SA, Italy

[§]Chemical and Life Sciences and Engineering, Kaust Catalysis Center, King Abdullah University of Science and Technology, Thuwal 23955-6900, Saudi Arabia

S *Supporting Information*

ABSTRACT: Theoretical studies on the overall catalytic cycle of isomerizing alkoxycarbonylation reveal the steric congestion around the diphosphine coordinated Pd-center as decisive for selectivity and productivity. The energy profile of isomerization is flat with diphosphines of variable steric bulk, but the preference for the formation of the linear Pd-alkyl species is more pronounced with sterically demanding diphosphines. CO insertion is feasible and reversible for all Pd-alkyl species studied and only little affected by the diphosphine. The overall rate-limiting step associated with the highest energetic barrier is methanolysis of the Pd-acyl species. Considering methanolysis of the linear Pd-acyl species, whose energetic barrier is lowest within all the Pd-acyl species studied, the barrier is

calculated to be lower for more congesting diphosphines. Calculations indicate that energy differences of methanolysis of the linear versus branched Pd-acyls are more pronounced for more bulky diphosphines, due to involvement of different numbers of methanol molecules in the transition state. Experimental studies under pressure reactor conditions showed a faster conversion of shorter chain olefin substrates, but virtually no effect of the double bond position within the substrate. Compared to higher olefins, ethylene carbonylation under identical conditions is much faster, likely due not just to the occurrence of reactive linear acyls exclusively but also to an intrinsically favorable insertion reactivity of the olefin. The alcoholysis reaction is slowed down for higher alcohols, evidenced by pressure reactor and NMR studies. Multiple unsaturated fatty acids were observed to form a terminal Pd-allyl species upon reaction with the catalytically active Pd-hydride species. This process and further carbonylation are slow compared to isomerizing methoxycarbonylation of monounsaturated fatty acids, but selective.
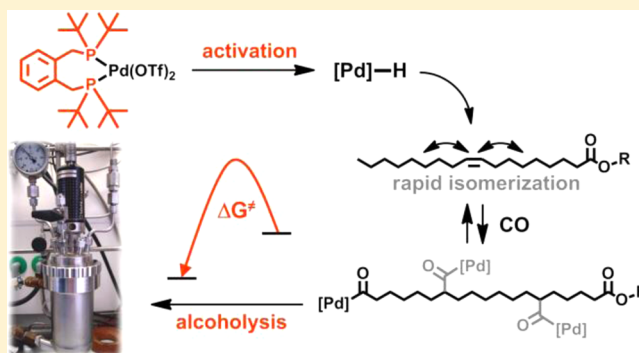
INTRODUCTION

The utilization of renewable resources as a source of chemicals requires their efficient transformation to useful building blocks. Fatty acids from plant oils are attractive substrates due to their unique long-chain methylene sequences.[1] Their incorporation into linear long-chain α,ω-functionalized compounds is of interest, for example, for the generation of semicrystalline aliphatic polyesters,[2] hydrophobic polyamides[2b] and hydrolytically degradable polyacetals.[3] The terminal functionalization of fatty acids is a synthetic challenge, however. Biotechnological[4] as well as entirely chemical catalytic approaches[5] are studied to this end. Self-metathesis of oleate can yield 1,18-octadecandioates (after subsequent hydrogenation of the double bond).[1b,5a,b] However, stoichiometric amounts of the C_{18}-alkene are formed. Also, as an equilibrium reaction only 50% conversion can be attained unless the product can be removed from the reaction mixture selectively.

By contrast, with their kinetically controlled nature selective isomerization/functionalization[5c,d,6] approaches in principle can incorporate the entire fatty acid chain. This is particularly difficult, however, as terminal olefins are thermodynamically strongly disfavored versus the internal double bonds of the substrate. The state of the art of isomerization/functionalization in terms of terminal selectivity and a lack of other undesired side reactions like olefin hydrogenation or further reactions of the products is isomerizing alkoxycarbonylation.[7] In this remarkable reaction, palladium(II) catalysts modified with electron rich, sterically demanding diphosphines like 1,2-$(CH_2P^tBu_2)_2C_6H_4$ (dtbpx)[8] convert the double bond deep in the chain of unsaturated fatty acids to a terminal ester group with high selectivity (up to >90%) and thus fully incorporate the fatty acid starting material into an α,ω-diester (Scheme

1).[2a,b,9] Notably not only pure oleate is converted, but also technical grade plant oils which are mixtures of fatty acids with

Scheme 1. Isomerizing Methoxycarbonylation of Plant Oils Generating Linear Long-Chain Diesters
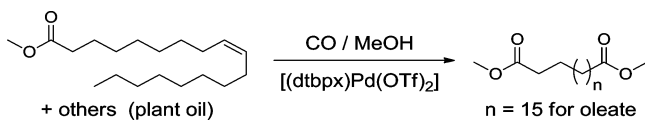
different numbers of carbon atoms and in particular multiple double bonds, and even pure linoleate is converted to linear diesters.

The perhaps most prominent isomerization/functionalization reaction to date is isomerizing hydroformylation.[10] For the isomerizing hydroformylation of methyl oleate, a selectivity of 40% has been achieved.[5c] Other than the isomerizing alkoxycarbonylation studied here, isomerizing hydroformylation is mostly catalyzed by trigonal bipyramidal rhodium complexes. The different nature and mechanism is also reflected in directly practically relevant features. Thus, the selectivity for linear products depends on the starting material (e.g., 1-octene results in higher linear selectivity than 2- or 4-octene) which is not the case for isomerizing alkoxycarbonylation (vide infra). In addition, side reactions like olefin hydrogenation and reduction of the generated products to alcohols are common, especially when functional ester groups are present in the substrate. It is worth noting that although the individual reactions of olefin isomerization and of hydroformylation have been studied extensively for numerous catalyst systems,[11] a mechanistic analysis of the overall catalytic cycle and reaction sequence does not exist for a catalyst capable of selective isomerizing hydroformylation.[10]

The same catalyst system as found to be efficient for isomerizing alkoxycarbonylation is used for the industrial production of methyl propionate by alkoxycarbonylation[11] of ethylene with CO and methanol.[12] This reaction has been deeply investigated and is well understood mechanistically.[8a,b,13] Isomerization and linear versus branched selectivity obviously do not apply here. Rates for this methoxycarbonylation of ethylene[8a] are substantially higher than rates for the isomerizing methoxycarbonylation of methyl oleate[2b] and methyl linoleate.[5a]

Cole-Hamilton and co-workers concluded from their study on the isomerizing methoxycarbonylation of octenes, that a hydride mechanism is operative and methanolysis is the rate-determining step.[7b] Our direct observations of stoichiometric isomerizing methoxycarbonylation of methyl oleate by low temperature NMR spectroscopy showed that under these conditions only linear product and one branched acyl, stabilized by chelated coordination of the substrates ester group form. Supported by DFT studies, this indicates that methanolysis is not only rate-determining, but also responsible for the selectivity of this remarkable transformation.[14] Recent findings suggest that steric congestion around the palladium center enhances productivity and selectivity of isomerizing alkoxycarbonylation.[15]

At this point, from these single pieces it is unclear how the overall transformation of isomerizing alkoxycarbonylation can be accounted for. Against this background, we now report a comprehensive mechanistic picture including the role of isomerization, and the origin of selectivity and reaction rates,

from a combined theoretical and experimental NMR and pressure reactor study. Relevant pathways to different branched byproducts are fully analyzed, which is a prerequisite for understanding and identifying the decisive structural features that make up a catalyst for this unique reaction. This analysis also provides for the first time an unravelling of a successful catalytic isomerization/functionalization scheme.

■ RESULTS AND DISCUSSION

Pressure Reactor Studies. To obtain data allowing for a quantitative comparison of the reaction of different substrates, preparative experiments with different olefins were performed in a 200 mL pressure reactor using 29.5 mmol of substrate and 0.8 mol % [(dtbpx)Pd(OTf)$_2$] as a catalyst precursor under 20 bar CO at 90 °C in neat methanol as a solvent and reagent. To gain insights into the role of isomerization under reaction conditions, a prior exposure of the olefinic substrate to the catalyst in the absence of CO was avoided. The catalyst was added into the loaded (substrate + methanol) and prepressurized (2 bar CO) reactor (for details cf. Supporting Information). Already at low conversions (e.g., ~15% for methyl oleate) isomerization of the substrate to the thermodynamic distribution of all isomers is observed, as evidenced by comparison with a genuine sample of the substrate with added [(dtbpx)Pd(OTf)$_2$] in methanol (Supporting Information). Note that during the entire catalytic transformation this distribution does not change and thus indicates that isomerization occurs, even in the presence of substantial amounts of CO (20 bar).

Average TOFs > 3,500 h^{-1} for ethylene, ca. 12 h^{-1} for methyl oleate and ca. 2 h^{-1} for methyl linoleate,[16] respectively, confirm the aforementioned higher productivity in ethylene methoxycarbonylation. Comparing rates of different mono-olefinic substrates (Figure 1) the conversion for shorter chain substrates is faster (ethylene > octenes > octadecene). Remarkably, the position of the double bond within the substrate virtually does not influence the rate (1-octene versus 4-octene).
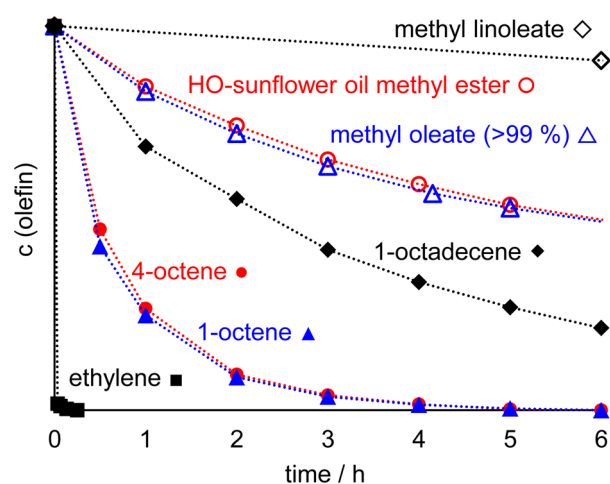

Figure 1. Conversion of different substrates in (isomerizing) alkoxycarbonylation in methanol as a solvent. Reaction conditions: 29.5 mmol olefin, 0.8 mol % [(dtbpx)Pd(OTf)$_2$], total volume 180 mL, 20 bar CO, 90 °C. Typical composition of HO-sunflower oil methyl ester: 92.5% methyl oleate (18:1); 2.5% methyl linoleate (18:2); 2.5% methyl palmitate (16:0); 1.5% methyl stearate (18:0); 1.0% methyl esters of longer chain (>C18) fatty acids.
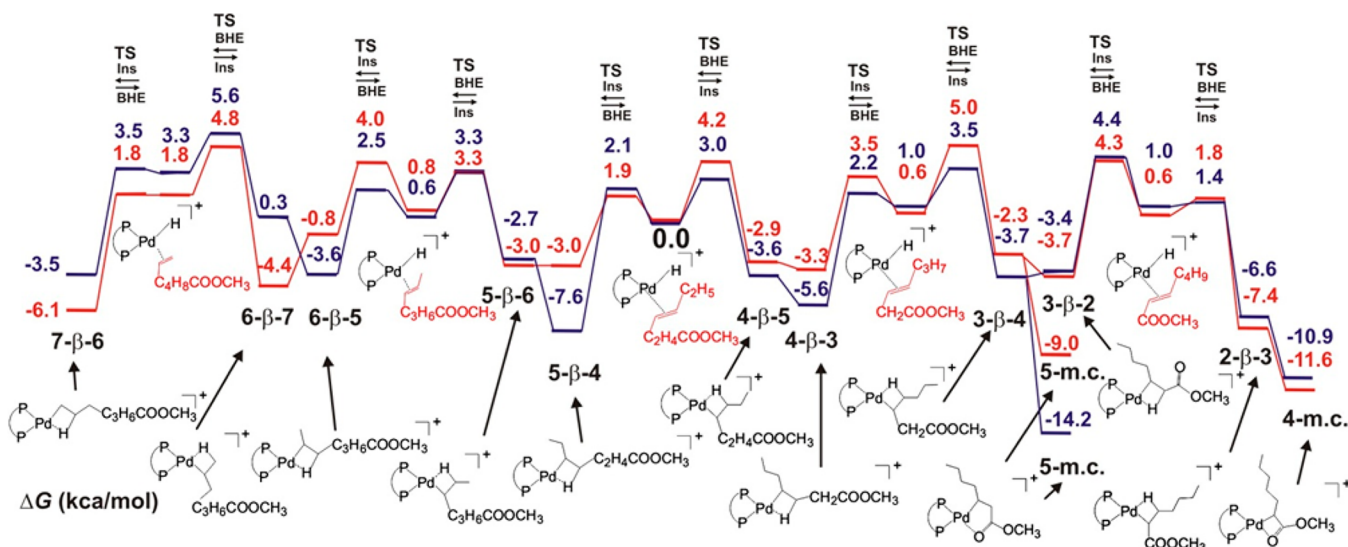
Figure 2. Energy profile (ΔG in kcal mol^{-1}) of isomerization along the hydrocarbon chain of the model substrate methyl heptenoate with the dtbpx (red line) and dmpx (blue line) coordinated diphosphine palladium(II) hydride species (relative to the energy of the Pd–H fragment with coordinated methyl 4-heptenoate as a reference point, set to zero).[23] "**X-β-Y**" indicates the respective Pd-Alkyl species,[24] "TS" the respective transition states, "BHE" the β-H elimination, and "Ins" the insertion reaction.

Selectivity for the different monoester products methyl nonanoate (95.0%), methyl 2-methyloctanoate (3.7%), methyl 2-ethylheptanoate (0.8%), and methyl 2-propylhexanoate (0.5%) is also identical for both octenes, thus indicating that isomerization is not the rate-limiting step. However, the length of the hydrocarbon chain of the substrate influences the overall rate. Note that for all substrates the selectivity does not change with time thus indicating that a conceivable decomposition of the catalyst does not influence the selectivity of isomerizing methoxycarbonylation.

Isomerization along the Hydrocarbon Chain. As isomerization is fast, even at temperatures of −80 °C,[14] experimental data alone is not conclusive in describing the overall energy profile of the isomerization reaction. DFT calculations starting from the diphosphine palladium(II) hydride fragment $[(P^\wedge P)Pd(H)]^+$ and methyl 4-heptenoate as model substrate were thus performed, calculating a series of insertion and subsequent β-hydride elimination reactions (Figure 2 and Supporting Information). These DFT calculations were performed with the Gaussian09 package[17] using the B3LYP[18] functional and the LANL2DZ ECP[19] with the associated valence basis set on the Pd-atom, and the 6-31G(d)[20] basis set on all the other atoms. All geometries were localized in the gas phase at the B3LYP level. Minima were localized by full optimization of the starting structures, while transition states were approached through a linear transit procedure starting from the coordination intermediate and then located by a full transition state search. All structures were confirmed as minimum or transition state through frequency calculations.[21] To gain insights into the influence of the catalysts' structure on catalysis, namely its steric repulsion around the metal center, the calculations were performed with the sterically demanding 1,2-$(CH_2P^tBu_2)_2C_6H_4$ (dtbpx) diphosphine and the less demanding 1,2-$(CH_2PMe_2)_2C_6H_4$ (dmpx) diphosphine (Chart 1).[22]

For both diphosphines the energetic profile of isomerization is relatively flat with barriers around 6−12 kcal mol^{-1}.[23] For both diphosphines, a chelated species is lowest in energy due to the electronically favored interaction of the substrates' ester

Chart 1. Diphosphine Palladium(II) Complexes with Different Steric Congestion around the Palladium Center Used for DFT Calculations of Isomerizing Alkoxycarbonylation

[(dmpx)Pd(L)(L')]   [(dtbpx)Pd(L)(L')]
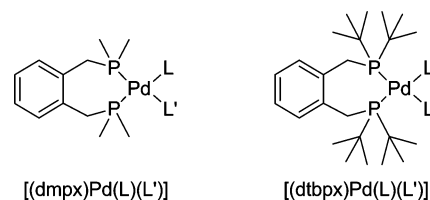
group with the metal center. The five-membered chelate (**5-m.c.**) is favored by 3.3 kcal mol^{-1} for the dmpx coordinated metal center, whereas in case of the sterically demanding dtbpx diphosphine the four-membered chelate (**4-m.c.**) is favored by 2.6 kcal mol^{-1} due to steric interactions of the diphosphines ^{t}Bu-groups with the alkyl chain of the substrate thus making a four-membered species more favorable although it may have higher ring strain within the chelate. Considering the other alkyl species (**3-β-2** to **7-β-6**)[24] the linear Pd-alkyl species **7-β-6** is favored by 1.7 kcal mol^{-1} over the methyl branched alkyl species **6-β-7** and over all other branched alkyl species by more than 2 kcal mol^{-1} for the bulky dtpbx diphosphine. This is not the case for the less bulky dmpx system where no preference for the linear alkyl species is found. The **5-β-4** alkyl species of the dmpx system is lowest in energy due to a favorable interaction of the substrates ester group with the β-hydrogen interacting with the metal center, thus making this alkyl species low in energy for this particular diphosphine Pd-alkyl species (cf. Supporting Information). Such an interaction of the substrates' ester group with a β-hydrogen is not observed for the more sterically demanding dtbpx system. Energy differences for the alkyl species can be directly traced to the specific nature of the metal center. For the bulky dtbpx system steric interactions are more pronounced than electronic interactions and vice versa for the less demanding dmpx system. Notably this is observed for the **6-β-7** versus **6-β-5** alkyl species: **6-β-7** with its interaction to a primary β-hydrogen is favored by 3.6 kcal

mol^{-1} for the case of dtbpx due to lower steric demand of the substrate around the metal center, while **6-β-5** is favored by 3.9 kcal mol^{-1} for the less demanding dmpx ligand due to the favored electronic interaction of a secondary β-hydrogen with the metal center versus the primary β-hydrogen interaction in **6-β-7** (Figure 2 and Supporting Information). From these studies of isomerization of methyl heptenoate along its hydrocarbon chain a preference for the formation of linear versus branched alkyl species is observed for sterically demanding ligands (dtbpx) which is not the case for less crowded diphosphines (dmpx). The former is in accordance with our aforementioned studies,[14] where the formation of a linear and a four-membered chelated species was observed when the catalytically active hydride species was exposed to methyl oleate. Notably, these calculations suggest that isomerization occurs with low barriers with either diphosphine.

Insertion of CO into Pd-Alkyl Species. CO insertion into the Pd-alkyl species was studied for both diphosphines starting from key alkyls, namely the four- (**4-m.c.**) and five- (**5-m.c.**) membered chelate, the linear Pd-alkyl **7-β-6**, the methyl branched alkyl **6-β-5** or **6-β-7** (depending on which of them is energetically favored) and the ethyl branched alkyl **5-β-4** (for complete details cf. Supporting Information).[25] Despite somewhat differing energies of the starting Pd-alkyl species due to chelating coordination of the substrates ester group (vide supra), barriers for CO insertion are only 8 to 18 kcal mol^{-1} and thus not prohibitive for the different linear and branched alkyls with both diphosphines. In general CO insertion is slightly exergonic. However, this energy released is not very high, such that CO insertion can be considered to be reversible. This agrees with experimental findings at low temperature for two selected alkyls.[14] The most notable difference observed is a generally more facile CO coordination with the less bulky diphosphine (dmpx).

However, both the decisive energy barriers ($\Delta G^{\ddagger}$) of CO insertion into the Pd-alkyl species and also the energetics (ΔG) of the overall CO insertion reaction are little affected by the diphosphine coordinated to the Pd-center and are thus in general little affected by the steric repulsion around the Pd-center. This was not only found by these theoretical studies but also experimentally by insertion of CO into diphosphine Pd-alkyl model compounds [(P^P)Pd(Me)Cl] with variable steric demanding diphosphines (vide infra).

Methanolysis of Pd-Acyl Species. As outlined, methanolysis is the rate-determining step of isomerizing methoxycarbonylation. For methanolysis of the linear Pd-acyl species [(P^P)PdC(=O)(CH$_2$)$_6$COOMe]$^+$ calculations suggest that a cluster of three methanol molecules is favored versus a single methanol coordinated transition state (TS) for the case of the bulky diphosphine (dtbpx).[26] Conversely, for all the branched alkyl species a single methanol coordinated transition state is calculated with lower energy versus the respective three methanol coordinated TS (Figure 5 and Figures S63 and S65). This change in the mechanism decisively contributes to the high selectivity with bulky diphosphines. In contrast for the less demanding dmpx diphosphine the three methanol cluster mechanism is calculated to be lower in energy for all Pd-acyl species (Figure S64). For both systems and mechanisms the lowest energies of methanolysis are calculated for the linear Pd-acyl species. However, the energetic barrier for methanolysis of the linear Pd-acyl is lower for the dtbpx coordinated species by $\Delta\Delta G^{\ddagger} = 3.0$ kcal mol^{-1} ($\Delta\Delta G^{\ddagger} = \Delta G^{\ddagger}_{dmpx} - \Delta G^{\ddagger}_{dtbpx} = 32.1-$
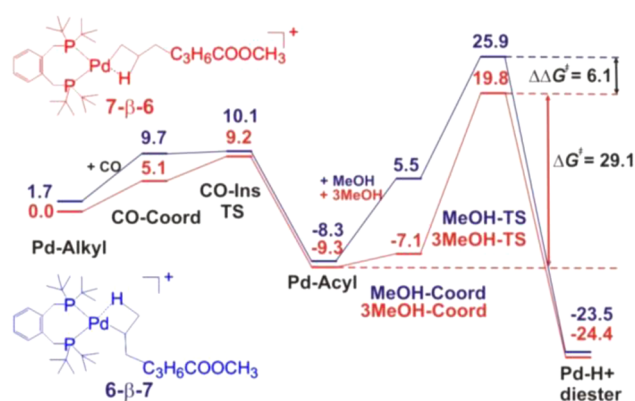

Figure 3. Energy profile (ΔG in kcal mol^{-1}) of CO insertion and subsequent methanolysis of the sterically congested dtbpx coordinated linear Pd-alkyl species (**7-β-6**; red line) and the methyl branched Pd-alkyl species (**6-β-7**; blue line), relative to the energy of the linear Pd-alkyl **7-β-6** as a reference point, set to zero.

Figure 4. Energy profile (ΔG in kcal mol^{-1}) of CO insertion and subsequent methanolysis of the dmpx coordinated linear Pd-alkyl species (**7-β-6**; red line) and the methyl branched Pd-alkyl species (**6-β-5**; blue line), relative to the energy of the linear Pd-alkyl **7-β-6** as a reference point, set to zero.
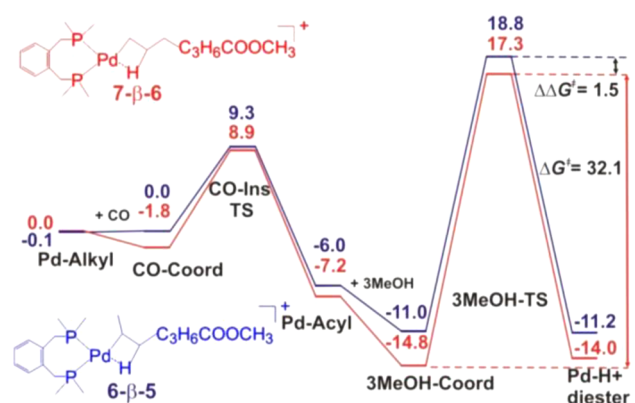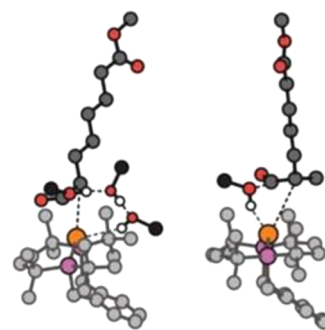

Figure 5. Transition states of linear (three-fold MeOH coordinated; left) versus methyl branched (single MeOH coordinated; right) Pd-acyl species.

29.1 kcal mol^{-1} in Figures 4 and 3), thus indicating significantly higher reaction rates for a more crowded Pd-center.[27]

For the dtbpx coordinated Pd-center, calculations indicate that methanolysis of the methyl branched Pd-acyl is lowest within the branched acyl species, but it is 6.1 kcal mol^{-1} higher in energy as compared to the linear analogue ($\Delta\Delta G^{\ddagger}$ in Figure 3). The highest energy was found for the methanolysis TS of the five-membered Pd-acyl species (formed by CO insertion

into the four-membered Pd-alkyl species), 9.4 kcal mol^{-1} higher than the linear Pd-alkyl (for a comparison of all pathways cf. Figure S65).

For the dmpx coordinated Pd-center, methanolysis of the Pd-acyl formed by insertion of CO into the five-membered Pd-alkyl to afford dimethyl 2-alkylsuccinate is calculated to be lowest within the branched Pd-acyl species but 1.2 kcal mol^{-1} higher than the TS of the linear Pd-acyl (for a comparison of all pathways cf. Figure S64). The highest barrier is found for the ethyl branched Pd-acyl species which is 4.8 kcal mol^{-1} higher as compared to the TS of the linear Pd-acyl (Figure S64). The TS of methanolysis of the methyl branched acyl species is calculated 1.5 kcal mol^{-1} higher as compared to the TS of the linear Pd-acyl ($\Delta\Delta G^{\ddagger}$ in Figure 4). The difference in the TSs energies is thus less pronounced than for the dtbpx coordinated species. Coming along with a change of the mechanism from a three methanol molecule cluster versus a single methanol molecule TS, these calculations indicate that energy differences in methanolysis TSs are less pronounced for the less demanding dmpx diphosphine. This overall picture suggests that the preference for the linear diester as the major product is not unique to the crowded dtbpx, but due to these differences the selectivity for the desired linear product is indeed higher.

Influence of the Substrate. In pressure reactor experiments (vide supra), conversion is faster for shorter chain substrates (average TOFs: > 3500 h^{-1} for ethylene, ca. 91 h^{-1} for 1-octene and 4-octene, and ca. 39 h^{-1} for 1-octadecene).[28] Selectivity to the linear product is 95% for the octenes and 90% for 1-octadecene and thus decreases with increasing length of the hydrocarbon chain. When comparing rates and selectivity of the conversion of octene versus octadecene, the overall reaction rate is ca. only half and the amount of branched side products twice as high for the longer chain substrate. Both observations may be due to different concentrations of the linear Pd-acyl, which is the starting point of the preferred further rate-determining methanolysis. A slight preference for the linear versus the numerous branched acyls ($\Delta\Delta G^{\ddagger} \geq 1$ kcal mol^{-1}) is calculated, but all will be equilibrated, such that for a longer chain substrate a larger part of the acyls will be present as less reactive branched acyls (Figure 3 and Supporting Information).

Comparing the rate of ethylene versus octene in (isomerizing) methoxycarbonylation, calculations indicate the higher rate of ethylene carbonylation is likely not only due to the occurrence of linear acyls exclusively, but also due to a significantly lower transition state of the rate-determining methanolysis step by $\Delta\Delta G^{\ddagger} = 9.7$ kcal mol^{-1} (Figure 6). This seems an intrinsic problem of the substrates' nature as formation of a Pd-alkyl is calculated to be more favored for Pd−H + ethylene versus Pd−H + 1-olefin, resulting in lower rates for (isomerizing) alkoxycarbonylation of higher olefins versus ethylene, although barriers of methanolysis of the respective Pd-acyls are similar for both substrates.

Experimental Studies on Diphosphine Structure. To probe these theoretical findings and to gain further insights on the influence of the diphosphines' structure on catalysis, a series of diphosphine palladium(II) ditriflate complexes [(P^P)Pd-(OTf)$_2$] and diphosphine palladium(II) methyl chloro complexes [(P^P)Pd(Me)Cl] with variable steric demand around the metal center were synthesized and evaluated (Chart 2, for diphosphine and complex synthesis cf. Supporting Information).
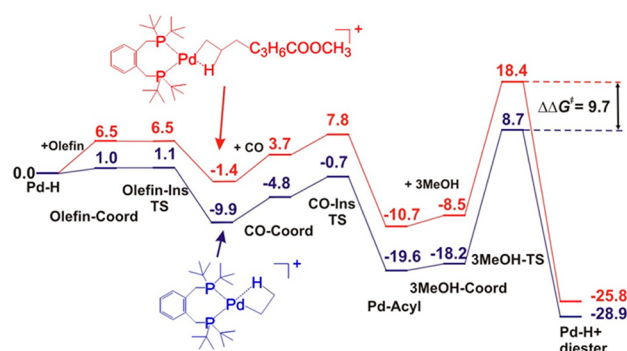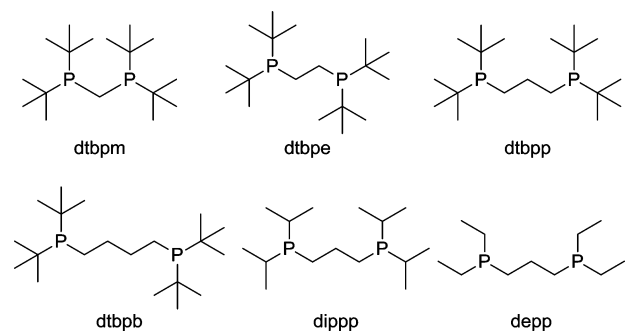

Figure 6. Energy profile (ΔG in kcal mol^{-1}) of ester formation starting from the Pd-hydride fragment [(dtbpx)Pd(H)]$^+$, ethylene and the longer chain olefinic substrate methyl 6-heptenoate (relative to the energy of the Pd-hydride fragment as a reference point, set to zero).

Chart 2. Diphosphines Evaluated in Isomerizing Methoxycarbonylation

Alkyl bridged diphosphines (P^P = R$_2$P(CH$_2$)$_n$PR$_2$; n = 1−4; R= ^{t}Bu, ^{i}Pr, Et) were used instead of 1,2-(CH$_2$PR$_2$)$_2$C$_6$H$_4$ diphosphines, as the former allow for more straightforward synthesis, and ^{t}Bu$_2$P(CH$_2$)$_3$P^{t}Bu$_2$ (dtbpp) is known to afford an active catalyst for isomerizing alkoxycarbonylation (and was also used for previous mechanistic NMR studies). Two approaches were followed to achieve variable steric demand around the metal center: the modification of the backbone of the diphosphines and the modification of the substituents on phosphorus. By increasing the number of bridging methylene units (C$_1$ to C$_4$; dtbpm, dtbpe, dtbpp, dtbpb) between two di-*tert*-butylphosphine moieties the space around the metal center decreases (vide infra). Modification of the substituents on phosphorus from *tert*-butyl to isopropyl and ethyl, respectively, with constant length of the bridge (C$_3$; dtbpp, dippp, depp), increases the available space (vide infra). The available space around the metal center was quantified by the opening angle at the metal center left open by the diphosphine in the respective Pd-complexes [(P^P)Pd(OTf)$_2$] (Table 1),[29] calculated from the respective X-ray crystal structures (for X-ray crystal structure analysis cf. Supporting Information). Larger values for the opening angle indicate less crowded metal centers. The experimental data show the tendency of the more sterically crowded metal centers [(dtbpp)Pd(OTf)$_2$] and [(dtbpx)Pd-(OTf)$_2$] to be more productive catalysts for isomerizing alkoxycarbonylation (Table 1).[30] All the other less crowded systems did not show any significant conversion of methyl oleate. Surprisingly [(dtbpb)Pd(OTf)$_2$] is also nonproductive although its steric congestion is almost equal to [(dtbpx)Pd-(OTf)$_2$].

Table 1. Opening Angle and Catalytic Results of Diphosphine Palladium(II) Ditriflate Complexes in Isomerizing Methoxycarbonylation of HO-Sunflower Oil Methyl Ester

| complex	opening angle [deg][c]	conversion of MO [%][f]	selectivity to linear diester [%][f]
$[(dtbpm)Pd(OTf)_2]^a$	213.4[d]	<0.5	n.d.
$[(dtbpe)Pd(OTf)_2]^a$	192.6	<0.5	n.d.
$[(dtbpp)Pd(OTf)_2]^a$	175.0[e]	25.4 (18 h) 70.6 (90 h)	82
$[(dtbpb)Pd(OTf)_2]^a$	172.8	<0.5	n.d.
$[(dippp)Pd(OTf)_2]^b$	197.6	<0.5	n.d.
$[(depp)Pd(OTf)_2]^b$	223.8	<0.5	n.d.
$[(dtbpx)Pd(OTf)_2]^a$	172.2[e]	94.8	91

[a]Reaction conditions: n(Pd) = 0.048 mmol; V(MO) = 2 mL; V(MeOH) = 8 mL; p(CO) = 20 bar; T = 90 °C; t = 90 h (for $[(dtbpp)Pd(OTf)_2]$: 18 and 90 h, for dtbpx: 18 h). [b]Reaction conditions: n(Pd) = 0.024 mmol; V(MO) = 1 mL; V(MeOH) = 4 mL; p(CO) = 20 bar; T = 90 °C; t = 90 h. [c]Opening angles were determined from X-ray crystal structure data as described in ref 29. [d]As no crystals suitable for X-ray diffraction of $[(dtbpm)Pd(OTf)_2]$ were obtained, data of $[(dtbpm)PdCl_2]$ was used. [e]Previously reported data from our group was used for $[(dtbpp)Pd(OTf)_2]$ (CCDC 893845) and $[(dtbpx)Pd(OTf)_2]$ (CCDC 817578). [f]Conversion and selectivity determined from GC of crude reaction mixture.

With regard to their observed lack of catalytic activity, complexes $[(dtbpm)Pd(OTf)_2]$, $[(dtbpe)Pd(OTf)_2]$ and $[(dtbpb)Pd(OTf)_2]$ were investigated in more detail. ^{1}H and ^{31}P NMR spectra of $[(dtbpm)Pd(OTf)_2]$ and $[(dtbpe)Pd-(OTf)_2]$ in methanol-d_4 or in a mixture of CD_2Cl_2/MeOH did not indicate the formation of any Pd-hydride species[31] (note that $[(dtbpp)Pd(OTf)_2]$ and $[(dtbpx)Pd(OTf)_2]$ cleanly yield a defined hydride species upon dissolution in methanol-d_4 or CD_2Cl_2/MeOH).[14,15] $[(dtbpb)Pd(OTf)_2]$ forms several non-identified Pd-hydride species, also underlined by addition of 20 equiv of methyl oleate to the NMR tube resulting in rapid isomerization (within 5 min) of the substrates' double bond to the equilibrium mixture of all isomers as observed for $[(dtbpp)Pd(OTf)_2]$ previously.[14] Addition of 20 equiv of methyl oleate to the methanol solution of $[(dtbpm)Pd(OTf)_2]$ showed no isomerization even after 12 h at room temperature. Only after heating to 90 °C for 90 min, isomerization to the equilibrium mixture was completed. With $[(dtbpe)Pd(OTf)_2]$ slow isomerization of methyl oleate (20 equiv) is observed already at room temperature, however, after 12 h at room temperature isomerization to the equilibrium mixture is not completed. Upon heating to 90 °C for 90 min, hydrogenation of the substrates' double bond to yield methyl stearate was observed.[32] These findings of olefin isomerization indicate the formation of certain amounts of Pd-hydride species for $[(dtbpm)Pd(OTf)_2]$ and $[(dtbpe)Pd(OTf)_2]$ although not directly observed by NMR spectroscopy; however, entry into the catalytic cycle may already be much less efficient for these catalyst systems.

To further probe the complexes' ability in isomerization, the above-mentioned experiments were performed in the presence of 6 equiv of CO.[33] $[(dtbpm)Pd(OTf)_2]$ did not show any isomerization in the presence of CO even at a temperature of 90 °C. $[(dtbpe)Pd(OTf)_2]$ showed no isomerization in the presence of CO at room temperature but at temperatures of 90 °C isomerization to the equilibrium mixture was observed within 2 h. However, the formation of methyl stearate was not

observed in the presence of CO. NMR analysis of the reaction mixture reveals the formation of a bridged hydrido-carbonyl species $[(dtbpe)Pd(\mu\text{-}H)(\mu\text{-}CO)Pd(dtbpe)]^+OTf^-$ (Scheme 2) as previously observed for $[(dtbpp)Pd(OTf)_2]$.[14] Addition

Scheme 2. Formation and X-ray Crystal Structure of the Hydrido-Carbonyl Bridged Species $[(dtbpe)Pd(\mu\text{-}H)(\mu\text{-}CO)Pd(dtbpe)]^+OTf^-$ from $[(dtbpe)Pd(OTf)_2]$ in the Presence of Methanol and CO^a
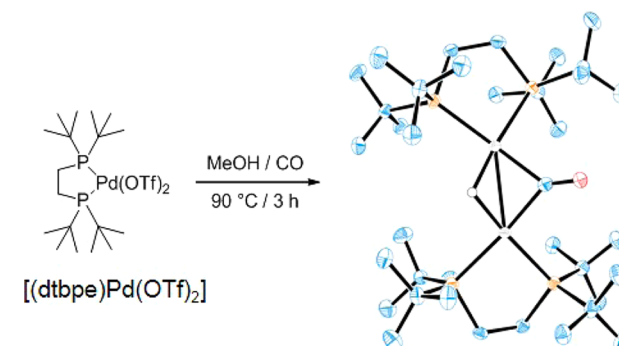
[a]Hydrogen atoms (except μ^2-H) and a noncoordinating triflate counterion were omitted for clarity. Displacement ellipsoids are shown at the 50% probability level.

of CO to a methanol-d_4 solution of $[(dtbpb)Pd(OTf)_2]$ resulted in quantitative formation of the deuterated diphosphine $(^tBu_2DP(CH_2)_4PD^tBu_2)(OTf)_2$ as evidenced in ^{31}P NMR spectra by a triplet at δ = 46.6 ppm with $^2J_{PD}$ = 70.2 Hz. Addition of methyl oleate to this solution did not result in any isomerization. Thus, the inactivity of $[(dtbpb)Pd(OTf)_2]$ in isomerizing alkoxycarbonylation is due to rapid decomposition of the catalytically active species in the presence of CO.[34]

To overcome the problem of less efficient hydride formation (vide supra) of $[(dtbpm)Pd(OTf)_2]$ and $[(dtbpe)Pd(OTf)_2]$ the methyl chloro complexes $[(dtbpm)Pd(Me)Cl]$, $[(dtbpe)-Pd(Me)Cl]$ and $[(dtbpp)Pd(Me)Cl]$ were used for isomerizing alkoxycarbonylation of the less challenging substrate 1-octene (Table 2). Note that these neutral diphosphine methyl chloro

Table 2. Catalytic Results of Diphosphine Palladium(II) Methyl Chloro Complexes in Isomerizing Methoxycarbonylation of 1-Octene

complex	conversion of 1-octene [%][b]	selectivity to methyl nonanoate [%][b]
$[(dtbpm)Pd(Me)Cl]^a$	5.7	73
$[(dtbpe)Pd(Me)Cl]^a$	33.8	92
$[(dtbpp)Pd(Me)Cl]^a$	96.1	90

[a]Reaction conditions: n(Pd) = 0.051 mmol; V(1-octen) = 1 mL (6.3 mmol); V(MeOH) = 4 mL; p(CO) = 20 bar; T = 90 °C; t = 90 h. [b]Conversion and selectivity determined from GC of crude reaction mixture.

complexes $[(P^\wedge P)Pd(Me)Cl]$ were used, as addition of AgOTf to generate the respective cationic complexes $[(P^\wedge P)Pd-(Me)]^+(OTf)^-$ instantaneously resulted in the formation of Pd-black. Dissociation of the chloro ligand is expected to be limited and thus hinders insertion reactions. The diphosphine ligand in turn may affect the ease of chloride dissociation. Consequently, observed rates with this system only allow for

qualitative conclusion concerning the effect of different diphosphines on the catalytic cycle.

The conversion of 1-octene increases with increasing steric demand of the diphosphine around the metal center which is in accordance with the results found in theoretical studies (vide supra). Differences in selectivity are less pronounced, in all cases the linear ester is the major product. For dtbpm, however, a significantly larger portion of the branched esters are formed, ~25% versus ~10% for the C$_2$- and C$_3$-backbone diphosphine. Note that isomerizing alkoxycarbonylation of methyl oleate was also performed with these methyl-chloro complexes (Supporting Information). Conversions slightly increased as compared to the respective ditriflate complexes, however, they are lower than for 1-octene.

The diphosphine palladium(II) methyl chloro complexes [(dtbpm)Pd(Me)Cl], [(dtbpe)Pd(Me)Cl] and [(dtbpp)Pd-(Me)Cl] were also used as model compounds to investigate the CO insertion into the Pd-alkyl species: an NMR tube was charged with the respective complex in CD$_2$Cl$_2$ and 1–3 equiv of ^{13}CO were added at 25 °C. Direct NMR spectroscopic measurements revealed that CO is inserted cleanly and completely within 5 min into the palladium(II) methyl species, generating the Pd-acyl species [(dtbpm)Pd(COMe)Cl], [(dtbpe)Pd(COMe)Cl], and [(dtbpp)Pd(COMe)Cl] which were characterized by NMR spectroscopy (Supporting Information). Note that also with an excess of CO the formation of a carbonyl coordinated cationic Pd-acyl species [(P^P)Pd(COMe)CO]$^+$(Cl)$^-$ was not observed.

The methanolysis of the Pd-acyl species was evaluated by generating [(dtbpm)Pd(COMe)Cl], [(dtbpe)Pd(COMe)Cl], and [(dtbpp)Pd(COMe)Cl] from the respective [(P^P)Pd-(Me)Cl] complexes in CD$_3$OD by addition of 2 equiv of ^{13}CO and direct observation of the methanolysis reaction after CO addition by ^{1}H NMR spectroscopy. [(dtbpp)Pd(Me)Cl] directly reacted to methyl acetate D$_3$CO(^{13}CO)Me, the deuterido-carbonyl bridged palladium(I) complex [(dtbpp)Pd-(μ-D)(μ-^{13}CO)Pd(dtbpp)]$^+$(Cl)$^-$, and the dichloro complex [(dtbpp)PdCl$_2$] within 5 min at room temperature (Supporting Information). Observation of the Pd-acyl species was not possible in methanol solution. By contrast [(dtbpe)Pd(Me)Cl] reacted to the observable acyl species [(dtbpe)Pd(COMe)Cl]. This acyl species reacts slowly with methanol at room temperature to methyl acetate D$_3$CO(^{13}CO)Me, the deuterido-carbonyl bridged palladium(I) complex [(dtbpe)Pd(μ-D)(μ-^{13}CO)Pd(dtbpe)]$^+$(Cl)$^-$, and the dichloro complex [(dtbpe)PdCl$_2$] (Supporting Information). [(dtbpm)Pd(Me)-Cl] also reacted to the acyl species [(dtbpm)Pd(COMe)Cl]. This acyl species was even less reactive toward methanol than the respective [(dtbpe)Pd(COMe)Cl] complex. Methanolysis was only observed at an elevated temperature of 50 °C.

These experimental findings demonstrate that, both the generation of the catalytically active Pd-hydride species is critical, but moreover the alcoholysis reaction of Pd-acyl species is influenced by the variable steric demand around the metal center which is in accordance with our theoretical findings.

Influence of the Alcohol. To study the influence of the alcohol on isomerizing alkoxycarbonylation, pressure reactor experiments in neat methanol, ethanol, n-propanol and isopropanol using 29.5 mmol of the respective oleate in a total volume of 180 mL and 0.8 mol % [(dtbpx)Pd(OTf)$_2$] as a catalyst precursor under 20 bar CO at 90 °C were performed (Figure 7).[35] Rates of conversion decrease within the series methanol > ethanol > n-propanol > isopropanol. Note that in
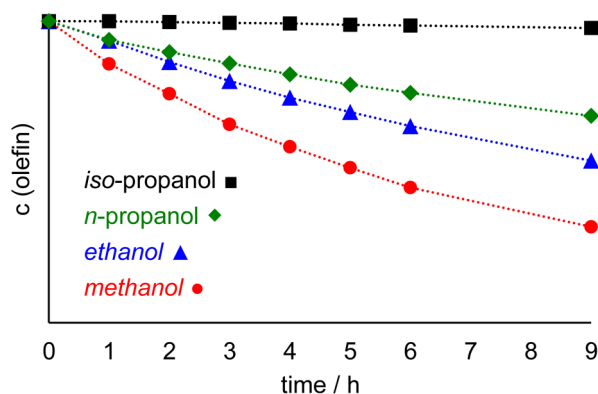

Figure 7. Isomerizing alkoxycarbonylation of isopropyl oleate in isopropanol (■, black), n-propyl oleate in n-propanol (◆, green), ethyl oleate in ethanol (▲, blue), and methyl oleate in methanol (●, red). Reaction conditions: 29.5 mmol oleate, 0.8 mol % [(dtbpx)Pd-(OTf)$_2$], total volume 180 mL, 20 bar CO, 90 °C.

these preparative experiments in neat alcohol as the reaction solvent the concentration of a lower molecular weight alcohol is always higher in a given volume,[36] resulting in higher productivity not only due to the higher reactivity of the alcohol, but also due to its' higher concentration. However, correcting the rates for the different alcohol concentrations still resulted in higher rates for methanol > ethanol > n-propanol > isopropanol.[37] Selectivities of 91 ± 1% were similar for methanol, ethanol and n-propanol and thus not significantly influenced by the alcohol.

To study the alcoholysis reaction itself, the dtbpx coordinated Pd-acyl species [(dtbpx)Pd(COMe)Cl] was generated in situ in an NMR tube by addition of 2 equiv of CO to a solution of [(dtbpx)Pd(Me)Cl] in 0.5 mL of CD$_2$Cl$_2$. Ten equiv of the respective alcohol (methanol, ethanol, n-propanol and isopropanol) were added and the alcoholysis reaction was followed by ^{1}H NMR spectroscopy. The rate of alcoholysis with methanol was fastest and already complete when the NMR tube was introduced into the probe after methanol addition. For the other alcohols the reaction was monitored over time showing that the rate of alcoholysis decreases within the series methanol > ethanol > n-propanol > isopropanol (Supporting Information). Theoretical studies on the alcoholysis reaction from the linear Pd-acyl [(dtbpx)PdC-(=O)(CH$_2$)$_6$COOMe]$^+$ with methanol and isopropanol, respectively, indicated that the energetic barrier of alcoholysis is higher for the sterically more demanding isopropanol versus methanol, and suggested a single molecule TS for isopropanol versus a three molecule cluster TS for methanol (vide supra).[38]

Multiple Unsaturated Fatty Acids. As outlined, plant oils inadvertently contain multiple unsaturated fatty acids in variable amounts. Thus, their role during catalysis must be accounted for. To this end, experiments under pressure reactor conditions (Figure 1 and Supporting Information) complemented by mechanistic studies with NMR spectroscopic methods were performed. As previously reported not only monounsaturated fatty acids (e.g., methyl oleate), but also multiple unsaturated fatty acids (e.g., methyl linoleate) are converted to the linear diesters by isomerizing alkoxycarbonylation (Scheme 1).[5a,39] The latter is of particular interest, as plant oils (e.g., rapeseed, sunflower, soybean or palm oil) are mixtures of fatty acids with different number of carbon atoms and double bonds.[1b] However, rates of methyl linoleate

alkoxycarbonylation are lower as compared to methyl oleate under identical reaction conditions as confirmed by TOFs of ca. 2 h^{-1} for neat linoleate versus ca. 12 h^{-1} for oleate (vide supra).

The selectivity to the linear diester is 45.5% and thus much lower as compared to methyl oleate where selectivities of >90% are observed. Compared to the isomerizing alkoxycarbonylation of methyl oleate, not only branched ester byproducts are formed, but also a triester, formed by double alkoxycarbonylation of the substrate, a methoxy substituted diester, formed by mono alkoxycarbonylation and hydromethoxylation of the remaining double bond of the substrate, and a C18 keto monoester product were identified by GC, NMR spectroscopy and ESI-MS (see also ref 39). In addition, the formation of a terminal dimethylacetal was observed by NMR spectroscopy. For detailed analysis and possible reaction pathways leading to the formation of these byproducts see the Supporting Information.

To gain mechanistic insights into the origin of the lower (versus methyl oleate) net overall rates, the catalyst precursor [(dtbpx)Pd(OTf)$_2$] was dissolved in CD$_3$OD, resulting in quantitative formation of the catalytically active deuteride species [(dtbpx)PdD(CD$_3$OD)]$^+$(OTf)$^-$ within 5 min at room temperature. Addition of stoichiometric amounts of methyl linoleate resulted in virtually quantitative formation of a disubstituted/internal Pd-allyl species [(dtbpx)Pd(η^3-C$_3$H$_3$)-{(CH$_2$)$_m$COOMe}{(CH$_2$)$_n$CH$_3$}]$^+$(OTf)$^-$ (n + m = 13).[40] This internal Pd-allyl species is isomerized virtually quantitatively to the monosubstituted/terminal Pd-allyl species [(dtbpx)Pd(η^3-C$_3$H$_4$){(CH$_2$)$_{14}$COOMe}]$^+$(OTf)$^-$ already at room temperature (Scheme 3 and Supporting Information).

Scheme 3. Reactivity of Stoichiometric Amounts of Methyl Linoleate with the Catalytically Active Deuteride Species [(dtbpx)PdD(CD$_3$OD)]$^+$ (n + m = 13; ΔG in kcal mol^{-1})
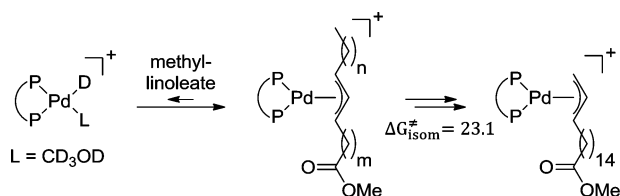
Kinetic observation of this transformation at temperatures between 25−55 °C yielded an overall energetic barrier of $\Delta G^{\ddagger}_{isom}$ = 23.1 kcal mol^{-1} for this isomerization (Supporting Information).

Insertion of carbon monoxide into the terminal Pd-allyl species was investigated using [(dtbpx)Pd(η^3-C$_4$H$_7$)]$^+$(OTf)$^-$ as a model substrate (for synthesis, characterization and X-ray crystal structure analysis of [(dtbpx)Pd(η^3-C$_4$H$_7$)]$^+$(OTf)$^-$ cf. the Supporting Information). At CO pressures of up to 5 bar in a pressure NMR tube in methylene chloride as the solvent, neither insertion nor coordination of CO was observed. Even at temperatures of 90 °C only decomposition of the Pd-species as indicated by the formation of Pd-black, free diphosphine and butadiene was observed. This is in stark contrast to the facile insertion of CO into Pd-alkyls, which is already observed at −80 °C.[14] Note that this observation does not necessarily reflect the CO insertion reaction rates only but also reflects the thermodynamic stability of the Pd-allyl species. When methanol was used as a solvent instead, under otherwise identical conditions, no reaction of the allyl was observed at room temperature, however after 3 days at 90 °C, the signals of the

starting material had disappeared completely. ^{13}C and ^{2}H NMR spectroscopy reveal the formation of deuterated dimethyl adipate, thus indicating insertion of CO, subsequent methanolysis to form methyl pentenoate, reinsertion of methyl pentenoate, isomerization, CO insertion and methanolysis to form dimethyl adipate (Supporting Information). These observations reflect the high thermodynamic stability of the allyl complexes and thus account for the lower reaction rates in isomerizing alkoxycarbonylation of methyl linoleate versus methyl oleate. However, as noted above small amounts (ca. 2.5%) of methyl linoleate in technical grade plant oils (Figure 1) do not significantly influence the overall rate of catalysis under pressure reactor conditions, presumably due to a certain entropic contribution and thus a strong influence of the temperature on the aforementioned equilibrium.

■ SUMMARY AND CONCLUSION

From these comprehensive theoretical and experimental studies the following picture evolves: Isomerization along the substrate hydrocarbon chain is associated with relatively low energy barriers for both diphosphine ligands studied to this end (Figure 2). Linear Pd-alkyls are more stable than branched alkyls for the very crowded metal centers. For sterically less encumbered analogues, their energies differ less. The vicinity of an ester group of the substrate can result in a slight stabilization of a branched agostic alkyl by an interaction of the functional group with a β-agostic hydrogen atom (however not to the extent that this renders the branched alkyl more stable than the linear alkyl for the sterically crowded metal center). More pronouncedly, coordination of the ester group itself can stabilize certain branched alkyls. A five-membered chelate can form (**5-m.c.**). For the sterically crowded metal center, a four-membered chelate is energetically more favorable (**4-m.c.**). In both cases, this chelate formed by coordination of the plant-oil derived ester group is more stable than all other alkyls. These theoretical results clearly show that isomerization itself is not the major rate-determining process. In the flat energy landscape with low barriers for interconversion, all alkyls are readily accessible energetically and are in equilibrium with each other.

For all the above alkyls, coordination of CO and subsequent insertion to form the respective Pd-acyls are energetically feasible and reversible. For the dtbpx coordinated metal center these organometallic species are in equilibrium with each other. Notwithstanding overall reaction rates can be influenced to a relevant extent by the portion in this equilibrium composition of a given species, namely, the linear Pd-acyl, which is the starting point of the preferred further rate-determining pathway (vide infra). This portion depends on statistics resulting from the chain length of the substrate, and (chelating) binding of a functional group present in the substrate. All these considerations are reflected in experimental monitoring of the progress of reaction over time for different substrates (all resulting in the linear ester as the major product): 4-octene reacts at virtually the same rate as 1-octene. 1-Octadecene with its larger number of methylene groups reacts slightly slower, and the rate of conversion of methyl oleate with its additional ester group is further slowed down.

The rate-determining step associated with the highest energetic barrier is invariably methanolysis of the Pd-acyl formed by carbon monoxide insertion (Figures 3 and 4). Considering methanolysis for the linear acyls, the barrier of methanolysis is decisively lower for a sterically encumbered metal site compared to active sites with less bulky diphosphine

ligands. This is due to a significantly higher stability of the methanol adducts for less bulky diphosphines. For bulky diphosphines, this ground state which precedes the rate-determining methanolysis step is destabilized. In fact, for bulky diphosphine ligands, its formation from the preceding direct product of CO insertion is not associated with a disadvantageously high energy gain. For less bulky ligands, the higher stability of the methanol adduct not only results in an effective higher barrier, but it can also render the overall methanolysis step thermoneutral. In addition, experimental studies suggest that an entry into a catalytic cycle may already be less efficient for such catalyst systems. Thus, hydrides are formed straightforwardly from dtbpx and dtbpp coordinated Pd-complexes in methanol, whereas this is not the case for less demanding diphosphines.

In view of the experimentally observed very high activity of ethylene methoxycarbonylation, and desirable enhanced rates of isomerizing methoxycarbonylation an analysis of the origin of these different rates is instructive. Theoretical studies confirm the transition state of methanolysis as the rate-determining step to be significantly lower for the case of ethylene versus a higher olefin, considering the entire reaction sequence starting from a Pd−H species. The overall energetic profile is lower for the case of ethylene (Figure 6). This can be traced back to a more facile insertion and a higher energy gain in the first metal−carbon bond forming step for ethylene. That is, the comparatively higher reactivity of ethylene in methoxycarbonylation appears to result from the intrinsically more favorable generation of an agostic ethyl from Pd−H + ethylene versus formation of a higher alkyl from Pd−H + 1-olefin rather than being brought about by a particular (diphosphine) ligand environment.

Another decisive consequence of the extreme steric bulk introduced by appropriate diphosphine ligands is a destabilization of the transition states of methanolysis for all branched acyls versus the linear acyl. In fact, the mechanism is calculated to change from a three molecule cluster TS in case of the linear Pd-acyl to a single molecule TS for all branched Pd-acyls. This accounts for the remarkable selectivity of isomerizing alkoxycarbonylation of methyl oleate. Even for the smallest branched alkyl with a methyl substituent on the carbonyl-bound carbon atom, which would result in a methyl-branched long-chain diester, the transition state for methanolysis is already significantly higher in energy. That the pathway to the linear product involves a cluster of three molecules of methanol in a concerted mechanism, while a pathway involving a single molecule of methanol is more favorable for the branched acyls only applies to the extremely bulky diphosphine-substituted catalysts, in other cases a "cluster-mechanism" is predicted to be operative also for the branched acyls.

Multiple unsaturated fatty acids, as exemplified by methyl linoleate, insert into the Pd−H species to form a Pd-allyl complex, which isomerizes to the terminal Pd-allyl, from which carbonylation occurs. Other than isomerization of the Pd-alkyl species formed from oleate, this isomerization is slow and associated with a significant energy barrier. However, the rate of carbonylation of this Pd-allyl is even lower, such that the major pathway is isomerization to the terminal allyl followed by carbonylation to the linear diester product. The remaining internal double bond is subject to further side reaction, alkoxycarbonylation to form a triester or hydromethoxylation. These are comparatively slow reactions, but due to the prolonged reaction times required to methoxycarbonylate the

allyl species they can occur on the product already formed and thus become relevant. However, the influence of small amounts ($\leq 2.5\%$) of methyl linoleate in technical grade plant oils is neglible. In preparative diester synthesis the use of methanol as the alcohol is desirable as its' concentration in a given volume is in general higher as compared to higher molecular weight alcohols and its' reactivity to the Pd-acyl species is higher compared to ethanol, n-propanol and isopropanol.

In summary, the steric demand around the Pd-center induced by the diphosphine ligand is both responsible for catalytic selectivity and productivity in isomerizing alkoxycarbonylation of plant oils. Sterically congested metal centers result in more selective catalysts as energy differences between the pathways leading to the linear versus the branched products of the rate-determining methanolysis steps are higher for these systems. Moreover these systems are more productive in general, as the energetic barrier of this rate-determining methanolysis step is lower as compared to less encumbered systems, which may not be active catalysts at all for methoxycarbonylation due to an unfavorable barrier. Concerning the isomerization step, our findings suggest that this is not a unique feature of sterically bulky diphosphines like dtbpx, but also other diphosphine Pd−H species can promote a rapid isomerization. However, formation of the Pd−H species from the catalyst precursor occurs much more readily for the bulky diphosphines, which may be a decisive factor.

From this first unraveling of a successful catalytic isomerization/functionalization reaction sequence, the following general picture emerges. The rate-determining step (in this case methanolysis) is preceded by a diverse relatively flat energy landscape of the various reversible reaction pathways (Curtin−Hammett kinetics). This applies to the isomerization sequences, but also to the first reaction steps of functionalization. Effectively, these isomerization/functionalization steps are in mutual equilibrium vice versa. Selectivity arises from differentiation of pathways in the final and highest barrier step of functionalization, here by extreme steric congestion about the active site. These features in our opinion define the essential prerequisite in designing isomerization/functionalization schemes with a single type of active sites, and this picture identified may also provide inspiration for multicomponent catalyst systems in which equilibrium landscapes may extend over the different cooperating types of sites.

■ ASSOCIATED CONTENT

ⓢ Supporting Information

Experimental and computational details, absolute energies (in Hartrees) of all molecules whose geometries were optimized, selected NMR spectra, selected GC traces and crystallographic details of [(dtbpm)PdCl$_2$] (CCDC 1010350), [(dtbpe)Pd-(OTf)$_2$] (CCDC 1010349), [(dtbpb)Pd(OTf)$_2$] (CCDC 1010347), [(dippp)Pd(OTf)$_2$] (CCDC 1010346), [(depp)Pd-(OTf)$_2$] (CCDC 1010345), [(dtbpe)Pd(μ-H)(μ-CO)Pd-(dtbpe)]$^+$OTf$^-$ (CCDC 1010348) and [(dtbpx)Pd(η^3-C$_4$H$_7$)]$^+$(OTf)$^-$ (CCDC 1010351). This material is available free of charge via the Internet at http://pubs.acs.org.

■ AUTHOR INFORMATION

Corresponding Authors

lcaporaso@unisa.it
stefan.mecking@uni-konstanz.de

■ REFERENCES

(1) (a) Biermann, U.; Bornscheuer, U.; Meier, M. A. R.; Metzger, J. O.; Schäfer, H. J. *Angew. Chem., Int. Ed.* **2011**, *50*, 3854−3871. (b) Chikkali, S.; Mecking, S. *Angew. Chem., Int. Ed.* **2012**, *51*, 5802−5808.

(2) (a) Quinzler, D.; Mecking, S. *Angew. Chem., Int. Ed.* **2010**, *49*, 4306−4308. (b) Stempfle, F.; Quinzler, D.; Heckler, I.; Mecking, S. *Macromolecules* **2011**, *44*, 4159−4166. (c) Vilela, C.; Silvestre, A. J. D.; Meier, M. A. R. *Macromol. Chem. Phys.* **2012**, *213*, 2220−2227. (d) Mutlu, H.; Hofsäß, R.; Montenegro, R. E.; Meier, M. A. R. *RSC Adv.* **2013**, *3*, 4927−4934. (e) Stempfle, F.; Ritter, B. S.; Mülhaupt, R.; Mecking, S. *Green Chem.* **2014**, *16*, 2008−2014.

(3) Chikkali, S.; Stempfle, F.; Mecking, S. *Macromol. Rapid Commun.* **2012**, *33*, 1126−1129.

(4) (a) Picataggio, S.; Rohrer, T.; Deanda, K.; Lanning, D.; Reynolds, R.; Mielenz, J.; Eirich, L. D. *Nat. Biotechnol.* **1992**, *10*, 894−898. (b) Schoerken, U.; Kempers, P. *Eur. J. Lipid Sci. Technol.* **2009**, *111*, 627−645. (c) Lu, W.; Ness, J. E.; Xie, W.; Zhang, X.; Minshull, J.; Gross, R. A. *J. Am. Chem. Soc.* **2010**, *132*, 15451−15455.

(5) (a) Stempfle, F.; Roesle, P.; Mecking, S. *ACS Symposium Series 1105 Biobased Monomers, Polymers and Materials*; Gross, R. A., Smith P. B., Eds.; American Chemical Society: Washington, D.C., 2012; pp 151−163. (b) Dinger, M. B.; Mol, J. C. *Adv. Synth. Catal.* **2002**, *344*, 671−677. (c) Behr, A.; Obst, D.; Westfechtel, A. *Eur. J. Lipid Sci. Technol.* **2005**, *107*, 213−219. (d) Ghebreyessus, K. Y.; Angelici, R. J. *Organometallics* **2006**, *25*, 3040−3044. (e) Deuss, P. J.; Barta, K.; de Vries, J. G. *Catal. Sci. Technol.* **2014**, *4*, 1174−1196.

(6) (a) Yuki, Y.; Takahashi, K.; Tanaka, Y.; Nozaki, K. *J. Am. Chem. Soc.* **2013**, *135*, 17393−17400. (b) van der Veen, L. A.; Kamer, P. C. J.; van Leeuwen, P. W. N. M. *Angew. Chem., Int. Ed.* **1999**, *38*, 336−338. (c) Selent, D.; Hess, D.; Wiese, K.-D.; Röttger, D.; Kunze, C.; Börner, A. *Angew. Chem., Int. Ed.* **2001**, *40*, 1696−1698. (d) Bronger, R. P. J.; Bermon, J. P.; Herwig, J.; Kamer, P. C. J.; van Leeuwen, P. W. N. M. *Adv. Synth. Catal.* **2004**, *346*, 789−799. (e) Klein, H.; Jackstell, R.; Wiese, K.-D.; Borgmann, C.; Beller, M. *Angew. Chem., Int. Ed.* **2001**, *40*, 3408−3411.

(7) (a) Pugh, R. I.; Drent, E.; Pringle, P. G. *Chem. Commun.* **2001**, 1476−1477. (b) Jiménez-Rodriguez, C.; Foster, D. F.; Eastham, G. R.; Cole-Hamilton, D. J. *Chem. Commun.* **2004**, 1720−1721.

(8) (a) Clegg, W.; Elsegood, M. R. J.; Eastham, G. R.; Tooze, R. P.; Wang, X. L.; Whiston, K. *Chem. Commun.* **1999**, 1877−1878. (b) Clegg, W.; Eastham, G. R.; Elsegood, M. R. J.; Heaton, B. T.; Iggo, J. A.; Tooze, R. P.; Whyman, R.; Zacchini, S. *Organometallics* **2002**, *21*, 1832−1840. (c) Carr, N.; Dunne, B. J.; Orpen, A. G.; Spencer, J. L. *J. Chem. Soc., Chem. Commun.* **1988**, 926−928.

(9) (a) Jiménez-Rodriguez, C.; Eastham, G. R.; Cole-Hamilton, D. J. *Inorg. Chem. Commun.* **2005**, *8*, 878−881. (b) Furst, M. R. L.; Le Goff, R.; Quinzler, D.; Mecking, S.; Botting, C. H.; Cole-Hamilton, D. J. *Green Chem.* **2012**, *14*, 472−477.

(10) Vilches-Herrera, M.; Domke, L.; Börner, A. *ACS Catal.* **2014**, *4*, 1706−1724.

(11) (a) van Leeuwen, P. W. N. M. *Homogeneous Catalysis: Understanding the Art*; Kluwer Academic Publishers: Dordrecht, 2004. (b) van Leeuwen, P. W. N. M.; Chadwick, J. C. *Homogeneous Catalysts: Activity−Stability−Deactivation*; Wiley-VCH Verlag GmbH & Co. KGaA: Weinheim, 2011.

(12) (a) McCoy, M.; Tremblay, J.-F. *Chem. Eng. News* **2009**, *87* (33), 9. (b) Harris, B. *Ingenia* **2010**, No. 45, 18−23.

(13) (a) Eastham, G. R.; Heaton, B. T.; Iggo, J. A.; Tooze, R. P.; Whyman, R.; Zacchini, S. *Chem. Commun.* **2000**, 609−610. (b) Frew,

J. J. R.; Damian, K.; Van Rensburg, H.; Slawin, A. M. Z.; Tooze, R. P.; Clarke, M. L. *Chem.—Eur. J.* **2009**, *15*, 10504−10513. (c) Clegg, W.; Eastham, G. R.; Elsegood, M. R. J.; Heaton, B. T.; Iggo, J. A.; Tooze, R. P.; Whyman, R.; Zacchini, S. *J. Chem. Soc., Dalton Trans.* **2002**, *17*, 3300−3308. (d) van Leeuwen, P. W. N. M.; Zuideveld, M. A.; Swennenhuis, B. H. G.; Freixa, Z.; Kamer, P. C. J.; Goubitz, K.; Fraanje, J.; Lutz, M.; Spek, A. L. *J. Am. Chem. Soc.* **2003**, *125*, 5523−5539.

(14) Roesle, P.; Dürr, C. J.; Möller, H. M.; Cavallo, L.; Caporaso, L.; Mecking, S. *J. Am. Chem. Soc.* **2012**, *134*, 17696−17703.

(15) Christl, J. T.; Roesle, P.; Stempfle, F.; Wucher, P.; Göttker-Schnetmann, I.; Müller, G.; Mecking, S. *Chem.—Eur. J.* **2013**, *19*, 17131−17140.

(16) TOFs were calculated from the data shown in Figure 1, from the data points at 2 min for ethylene, at 5 h for methyl oleate and at 6 h for methyl linoleate, respectively.

(17) Frisch, M. J.; Trucks, G. W.; Schlegel, H. B.; Scuseria, G. E.; Robb, M. A.; Cheeseman, J. R.; Scalmani, G.; Barone, V.; Mennucci, B.; Petersson, G. A.; Nakatsuji, H.; Caricato, M.; Li, X.; Hratchian, H. P.; Izmaylov, A. F.; Bloino, J.; Zheng, G.; Sonnenberg, J. L.; Hada, M.; Ehara, M.; Toyota, K.; Fukuda, R.; Hasegawa, J.; Ishida, M.; Nakajima, T.; Honda, Y.; Kitao, O.; Nakai, H.; Vreven, T.; Montgomery, J. A., Jr.; Peralta, J. E.; Ogliaro, F.; Bearpark, M.; Heyd, J. J.; Brothers, E.; Kudin, K. N.; Staroverov, V. N.; Kobayashi, R.; Normand, J.; Raghavachari, K.; Rendell, A.; Burant, J. C.; Iyengar, S. S.; Tomasi, J.; Cossi, M.; Rega, N.; Millam, J. M.; Klene, M.; Knox, J. E.; Cross, J. B.; Bakken, V.; Adamo, C.; Jaramillo, J.; Gomperts, R.; Stratmann, R. E.; Yazyev, O.; Austin, A. J.; Cammi, R.; Pomelli, C.; Ochterski, J. W.; Martin, R. L.; Morokuma, K.; Zakrzewski, V. G.; Voth, G. A.; Salvador, P.; Dannenberg, J. J.; Dapprich, S.; Daniels, A. D.; Farkas, Ö.; Foresman, J. B.; Ortiz, J. V.; Cioslowski, J.; Fox, D. J. *Gaussian 09*; Gaussian, Inc.: Wallingford, CT, 2009.

(18) Becke, A. D. *J. Chem. Phys.* **1993**, *98*, 5648−5652.

(19) (a) Dunning, T. H., Jr.; Hay, P. J. In *Modern Theoretical Chemistry*; Schaefer, H. F., III, Ed.; Plenum: New York, 1976; pp 1−28. (b) Hay, P. J.; Wadt, W. R. *J. Chem. Phys.* **1985**, *82*, 270−283.

(20) (a) Ditchfield, R.; Hehre, W. J.; Pople, J. A. *J. Chem. Phys.* **1971**, *54*, 724−728. (b) Hehre, W. J.; Ditchfield, R.; Pople, J. A. *J. Chem. Phys.* **1972**, *56*, 2257−2261. (c) Hariharan, P. C.; Pople, J. A. *Mol. Phys.* **1974**, *27*, 209−214. (d) Gordon, M. S. *Chem. Phys. Lett.* **1980**, *76*, 163−168. (e) Hariharan, P. C.; Pople, J. A. *Theor. Chim. Acta* **1973**, *28*, 213−222.

(21) Note that single point energy calculations with the triple-ζ plus polarization TZVP basis set were performed on selected Pd-alkyl species (**5-β-4**, **5-β-6** and **7-β-6**; cf. the Supporting Information) to validate the chemical scenario derived with the 6-31G(d) basis set.

(22) In the isomerization study calculations on *cis-* and *trans-*isomers of the respective olefins were performed for each coordination and transition state. The results reported herein refer to the energetically favored *trans-*isomer path for both diphosphines.

(23) The coordination energy of methyl 4-heptenoate to the Pd-H fragment to form the olefin coordinated [(diphosphine)PdH(olefin)]$^+$ complex is ΔG = 7.6 kcal mol^{-1} for the dtbpx coordinated species and ΔG = −5.5 kcal mol^{-1} for the dmpx coordinated species.

(24) In the **X-β-Y** notation, the first number (X) denotes the carbon atom attached to the Pd-center, the second number (Y) denotes the carbon atom whose hydrogen atom interacts with the fourth coordination site of the Pd-center via a β-hydrogen interaction.

(25) Energies of the four- and five-membered chelate have been reported for both the dtbpx and dmpx coordinated diphosphine previously by us. The energy of the linear Pd-Alkyl **7-β-6** of the dtbpx coordinated species has been reported. CO insertion and methanolysis has been reported for the four-membered (**4-m.c.**) and the linear **7-β-6** dtbpx coordinated species (cf. ref 14).

(26) The methanolysis reaction of the linear and the five-membered chelate dtbpx coordinated Pd-acyl species has been reported previously (cf. ref 14).

(27) $\Delta\Delta G^{\ddagger}$ = 3.0 kcal mol^{-1} refers to the three methanol coordinated TSs. For the single methanol coordinated TSs $\Delta\Delta G^{\ddagger}$ = 0.7 kcal mol^{-1}

J

dx.doi.org/10.1021/ja508447d | *J. Am. Chem. Soc.* XXXX, XXX, XXX−XXX

is calculated, thus also indicating higher reaction rates for the more crowded diphosphine.

(28) TOFs were calculated from the data shown in Figure 1, from the data points at 2 min for ethylene and at 1 h for 1-octene, 4-octene and 1-octadecene, respectively.

(29) The opening angle describes a cone at the metal center, which is defined by the space left open by the diphosphine not occupied by any of its atoms. It amounts to twice the half-cone angle as defined in ref 15.

(30) Note that the dmpx ligand used for the DFT calculations has an opening angle of 219.5° (calculated from the quarternary carbon atoms of $[(dtbpx)Pd(OTf)_2]$) and is thus similarly congesting as $[(dtbpm)Pd(OTf)_2]$.

(31) Formation of hydride species is indicated in ^1H NMR spectroscopy by signals in the range of 0−30 ppm and in ^{31}P NMR spectroscopy by appearance of pairs of doublets indicating unsymmetrical substituted square planar Pd-centers.

(32) Hydrogenation may occur via Pd-catalyzed transfer hydrogenation with methanol as the hydrogen source.

(33) The respective complex was dissolved in methanol-d_4 or CD_2Cl_2/MeOH respectively, and 6 equiv of CO were added via syringe into the NMR tube. Afterwards 20 equiv of methyl oleate were added.

(34) Note that under preparative conditions, the protonated diphosphine was also observed after a carbonylation experiment.

(35) Quantitative conversion of $[(dtbpx)Pd(OTf)_2]$ to the respective $[(dtbpx)PdH(R-OH)]^+$ species and rapid isomerization of the respective oleates with these Pd-H species was evidenced by NMR spectroscopy (cf. Supporting Information).

(36) In a total volume of 180 mL concentrations are 0.164 M oleate, 23.3 M methanol, 16.1 M ethanol, 12.5 M n-propanol, 12.2 M isopropanol.

(37) Rate constants assuming first order reactions in oleate are: $k_{MeOH} = 3.7 \times 10^{-5}$ s^{-1}; $k_{EtOH} = 2.0 \times 10^{-5}$ s^{-1}; $k_{n-PrOH} = 1.2 \times 10^{-5}$ s^{-1}; $k_{isoPrOH} = 7.1 \times 10^{-7}$ s^{-1}.

(38) For the three molecule cluster TSs $\Delta G^{\ddagger}_{methanol} = 29.1$ kcal mol^{-1} and $\Delta G^{\ddagger}_{isopropanol} = 48.4$ kcal mol^{-1} were calculated. For the single molecule TSs $\Delta G^{\ddagger}_{methanol} = 34.5$ kcal mol^{-1} and $\Delta G^{\ddagger}_{isopropanol} = 38.2$ kcal mol^{-1} were calculated.

(39) Furst, M. R. L.; Seidensticker, T.; Cole-Hamilton, D. J. Green Chem. 2013, 15, 1218−1225.

(40) This differs from the behavior of monounsaturated olefins (e.g., methyl oleate) where the equilibrium between Pd-D + olefin and Pd-alkyl is on the side of the Pd-D species under these conditions.